Surface Mesohighs and Mesolows

Richard H. Johnson
Department of Atmospheric Science, Colorado State University, Fort Collins, Colorado

ABSTRACT

Through detailed and remarkably insightful analyses of surface data, Tetsuya Theodore Fujita pioneered modern mesoanalysis, unraveling many of the mysteries of severe storms. In this paper Fujita's contributions to the analysis and description of surface pressure features accompanying tornadic storms and squall lines are reviewed.

On the scale of individual thunderstorm cells Fujita identified pressure couplets: a mesolow associated with the tornado cyclone and a mesohigh in the adjacent heavy precipitation area to the north. On larger scales, he found that squall lines contain mesohighs associated with the convective line and wake depressions (now generally called wake lows) to the rear of storms. Fujita documented the structure and life cycles of these phenomena using time-to-space conversion of barograph data.

Subsequent investigations have borne out many of Fujita's findings of nearly 50 years ago. His analyses of the surface pressure field accompanying tornadic supercells have been validated by later studies, in part because of the advent of mobile mesonetworks. The analyses of squall-line mesohighs and wake lows have been confirmed and extended, particularly by advances in radar observations. These surface pressure features appear to be linked to processes both in the convective line and attendant stratiform precipitation regions, as well as to rear-inflow jets, gravity currents, and gravity waves, but specific roles of each of these phenomena in the formation of mesohighs and wake lows have yet to be fully resolved.

1. Introduction

In Japan in the late 1940s Tetsuya Theodore Fujita carried out his first detailed analyses of surface weather systems. Inspired by observations of dramatic surface weather changes during the passage of thunderstorms, tornadoes, and even a solar eclipse, he developed in just a few short years an array of techniques for the analysis of subsynoptic weather phenomena. These efforts led to new insights into atmospheric processes on the largely unstudied scale of local weather. Fujita's early investigations, along with subsequent work at the University of Chicago in the early 1950s, marked the birth of mesometeorology. The mesoanalysis techniques that he developed then formed the foundation of subsequent mesoscale research.

Very early on, Fujita saw the largest signal in surface weather patterns occurred in connection with deep convection. This observation led him to direct much of his initial attention to severe local storms, an interest that continued throughout his career.

In this paper Fujita's early studies of convective storms and their associated surface effects are reviewed. Specific emphasis is given to surface mesoscale pressure fields associated with severe convective weather, notably mesohighs and mesolows. In addition, we examine how recent studies have substantiated many of Fujita's early discoveries and shed new light on this subject. Much of the chronology

Richard H. Johnson

Corresponding author address: Richard H. Johnson, Department of Atmospheric Science, Colorado State University, Fort Collins, CO 80523.
E-mail: rhj@atmos.colostate.edu
In final form 22 June 2000.

of Fujita's work can be found in his 1992 memoirs (Fujita 1992).

2. Fujita's first mesoanalyses

In 1947, just one year after choosing "weather science" as a career and three years prior to receiving a doctor of science degree from Tokyo University, Fujita developed a keen interest in the effects of convection on surface weather. His initial interest in this subject arose from noting that the direction and speed of local winds during convective storms were entirely different from those inferred from large-scale synoptic charts. On 24 August 1947 he had an opportunity to directly observe a thunderstorm from a station atop 1054-m-high Seburiyama Mountain in Kyushu. From station pressure measurements, computations of the hydrostatic pressure, and corrections for suction effects of the building in the wind, he was able to compute nonhydrostatic pressure near cloud base and infer the existence of a strong downward current in the thunderstorm. At the time, the existence of such a current in thunderstorms was a novel idea in Japan and not widely accepted. Nevertheless, his observations led him to postulate a now impressively realistic thunderstorm model (Fig. 1) that was published several years later (Fujita 1951). Fujita analyzed a series of surface pressure maps for this case using pressure traces from 30 stations (Fig. 2). Based on a time-to-space conversion of the pressure data, he was able to depict a number of rapidly evolving thunderstorm highs 20–100 km in the horizontal dimension. Since the rise–fall pressure tendencies had the appearance of a human nose, he referred to the high pressure associated with the thunderstorm as a thunder-nose. The maps in Fig. 2 represent Fujita's first mesoanalysis charts, although at the time he referred to this local analysis as microanalysis.

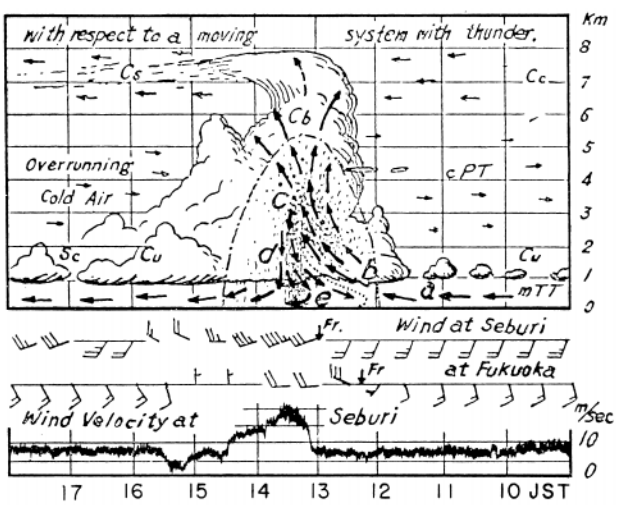

FIG. 1. Model of the Seburiyama thunderstorm of 24 Aug 1947 (Fujita 1951). Fujita (1992) noted that, "this model was produced in March 1949, leading to a presentation in Japanese on May 6, 1949. An English translation was sent to Dr. Byers on December 5, 1950."

Serendipitously, after a talk on the thunder-nose in Kyushu in 1949, someone pointed out to Fujita that a paper by Horace R. Byers (1942) on nonfrontal thunderstorms had been found in a wastepaper basket at the Seburiyama Mountain station. Realizing its connection with his own work, Fujita sent two of his papers to Byers at the University of Chicago. Byers was particularly impressed with the analysis of the Seburiyama thunderstorm and the conclusions regarding the importance of the thunderstorm downdraft, conclusions that he had reached independently as a result of the 1946–47 Thunderstorm Project (Byers and Braham 1949). This correspondence led to Fujita's eventual move to the University of Chicago in 1953, where he began his mesoanalysis research in the United States.

3. Mesoanalyses of severe storms in the United States—Fujita's next decade

In 1951 a special observing network was established in the central plains in support of the research activities of the Severe Local Storms Research Unit of the U.S. Weather Bureau. The scale of the network was unprecedented: by 1953 nearly 200 stations (including both regularly reporting and special sites) spaced at ~50 km were deployed over all or parts of six states—the most extensive mesonetwork ever established. The microbarographs, hygrothermographs, thermographs, and wind and rainfall observations from special sites presented a golden opportunity for Fujita, who had just arrived in the United States from Japan armed with an arsenal of techniques for data reduction and mesoanalysis used in his study of cold fronts, severe storms, and typhoons in Japan, along with new techniques being developed in the United States.

Some of the first results of the analysis of summer 1953 mesonetwork data were reported in a landmark paper (Fujita 1955). Using time-to-space conversion of the barograph traces, Fujita constructed detailed

mesoanalyses of the pressure field accompanying squall lines. This work led to the development of a conceptual model for the squall-line surface pressure field (Fig. 3), wherein three principal features of the pressure field were identified: the pressure surge, the thunderstorm high [referred to in Fujita et al. (1956) as a mesohigh], and the wake depression. Fujita attributed the pressure surge and thunderstorm high to evaporation of precipitation in downdrafts, as illustrated in Fig. 4. This mechanism for the thunderstorm high had been proposed earlier (Humphreys 1929; Suckstorff 1935), wherein the former it was argued that the frictional retardation of the surface outflow from evaporatively driven downdrafts was an important factor in the increase of surface pressure. There was some controversy in the early to mid-1940s about the role of dynamical effects (e.g., nonhdrostatic pressure rise due to the impact of the downdraft with the ground) on production of the thunderstorm high (see Sawyer 1946 for a discussion), but results from the Thunderstorm Project (Byers and Braham 1949) and computations carried out by Fujita (1959) indicated that the primary contributor to the surface cold dome is evaporation of rainfall below cloud base. However, Fujita also noted that an additional pressure rise of ~1–2 mb could occur in the heavy rain directly beneath the downdraft due to nonhydrostatic effects, a feature he referred to as the pressure nose (Fujita 1963). Fujita (1959) also speculated that melting snow or hail could also contribute to the surface mesohigh, an idea later confirmed and quantified by Atlas et al. (1969).

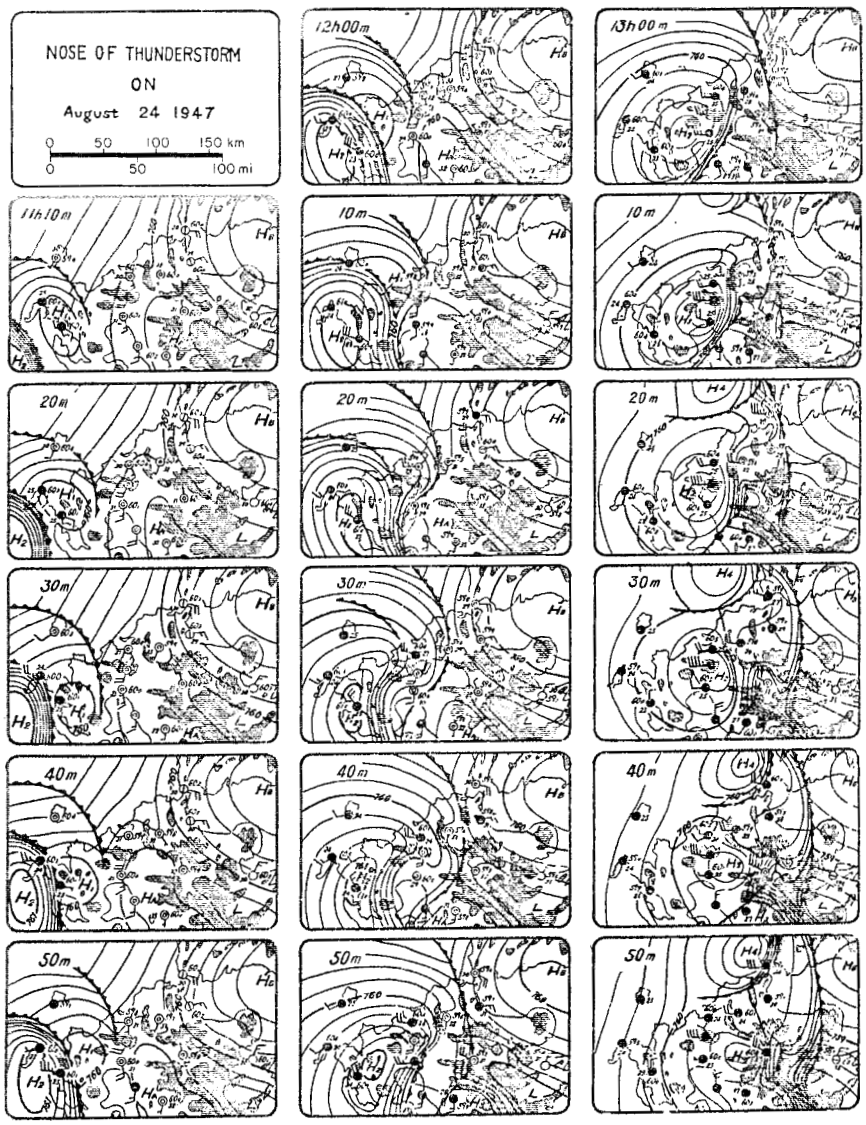

FIG. 2. Microanalysis of the thunder-nose of 24 Aug 1947 (Fujita 1951). This is the first sequence of mesoanalysis maps produced by Fujita. In order to create this map, Fujita visited individual weather stations to hand copy recorded traces on tracing paper. No center for national data archive nor copying machine was available in Japan in the 1940s.

Fujita (1955) initially explained the wake depression as a dynamical response to storm-relative front-to-rear flow around the cold dome (open arrows in Fig. 4), much like low pressure produced due to flow separation in the wake of a blunt body. If the low-level flow relative to the cold dome were reversed, then, Fujita argued, the wake depression would be found ahead of the thunderstorm. However, later Fujita (1963) retracted these ideas on the basis that the horizontal dimensions of the mesohigh are too large to permit the development of the wake flows shown in Fig. 4. He thus recommended abolishment of the term wake depression and recommended the use of mesodepression for the lack of a more suitable term. Subsequent research (to be discussed later) has shed new light on mechanisms for mesoscale low pressure perturbations associated with squall lines.

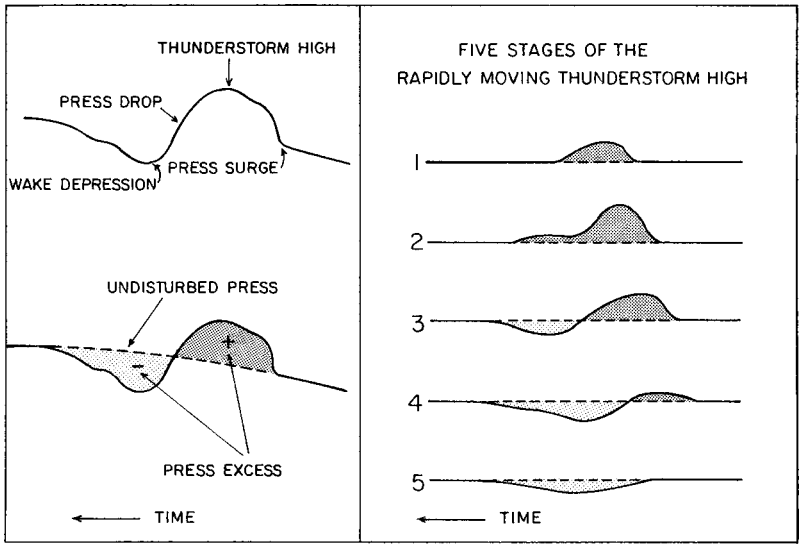

FIG. 3. (left) Profile of the pressure disturbance through the center of a rapidly moving squall line and definitions of pressure features. (right) Five stages of the pressure field: 1) initiation stage, 2) development stage, 3) mature stage, 4) dissipation stage, and 5) remnant stage. Redrafted from Fujita (1955).

Also shown in Fig. 3 are typical pressure profiles for various stages in the life cycle of a squall line. According to Fujita (1955, 1963), a squall mesosystem develops as a small mesohigh and dissipates as a mesodepression after going through five stages:

1) initiation stage—a small mesohigh, which can be detected only by a (meso)network, forms and develops;
2) development stage—horizontal dimensions increase to over 100 mi, yet no mesodepression appears inside the system;
3) mature stage—showers reach their maximum intensities, and a mesodepression develops behind them;
4) dissipation stage—the mesodepression reaches its minimum pressure and showers disintegrate; and
5) remnant stage—the mesohigh flattens out, and the mesodepression fills.

The first four of these stages are depicted in Fig. 5 (from Fujita 1963) for three different modes of development: on the cold side of a front, along a front, and on the warm side of a front. The disturbance in each case has the same pressure anomaly pattern, but the differing background pressure fields lead to different appearances in the total pressure fields.

While analyzing the 1953 mesonetwork data, Fujita was aware that several different scales of convectively generated, surface pressure disturbances existed. On the largest scales were those associated with squall mesosystems containing multiple thunderstorm cells, such as those described above, while on the smallest scales pressure disturbances accompanied individual thunderstorms. This distinction was brought out in a study of the severe weather outbreak of 24–25 June 1953 (Fujita et al. 1956). This paper dealt with severe storms that accompanied the passage of a cold front over the central United States. From synoptic to mesoscale analyses for this case, Fujita et al. (1956) identified three types of mesoscale pressure phenomena: the mesohigh, the pressure jump line, and the pressure couplet.

The mesohigh of Fujita et al. (1956) is synonymous with the thunderstorm high discussed previously. An example is shown in Fig. 6 along the Kansas–Nebraska border at 0200 central standard time (CST) on 25 June 1953. This mesohigh was several hundred kilometers long, trailed by a low pressure area. The gradient between high and low pressure was intense, ~10 mb $(80\ \text{km})^{-1}$.

A pressure jump line, originating from a previous convective system in northeastern Kansas, was analyzed in southeastern Kansas (Fig. 6). Parts of it were well separated from the cold front to the north. Fujita et al. (1956) noted no precipitation and only scattered-to-broken clouds associated with this feature. Similar pressure jumps were analyzed at the time by Williams (1948, 1953) and initially attributed to hydraulic jump dynamics by Tepper (1950) and later to nonlinear geostrophic adjustment to momentum forcing by Tepper (1955). Later work suggests that the pressure jump lines are in many cases surface manifestations of undular bores (Simpson 1987), which arise from an impulsive forcing such as a downdraft impinging upon a stable layer (e.g., the nocturnal inversion) or a gravity current (e.g., a thunderstorm outflow) intruding on a stable layer.

The pressure couplet was defined as a high pressure area and adjacent low pressure area of similar magnitudes and intensities. Fujita noted that the worst weather (e.g., tornadoes) appeared to be associated with the low pressure part of the couplet. In fact, he associated this part with the tornado cyclone, a term introduced by Brooks (1949) to describe the low pres-

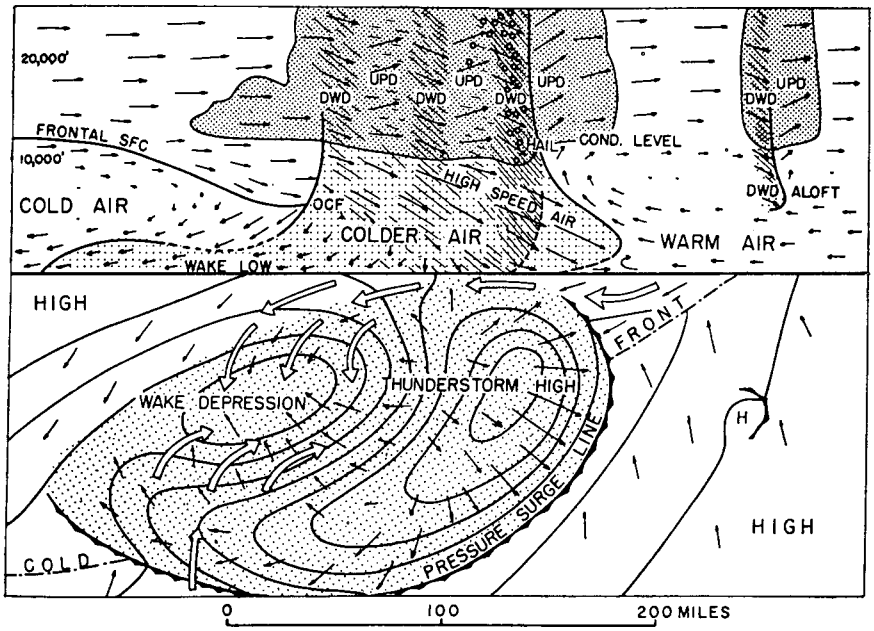

FIG. 4. Fujita's early model of squall-line circulation: DWD = downdraft, UPD = updraft. From Fujita (1955).

mesodepressions—an analogy to obstacle flow—was incorrect; however, he did not offer an alternative explanation. At about the same time, Pedgley (1962) had analyzed a squall line passing over England on 28 August 1958 that had the same characteristic surface pressure patterns reported by Fujita (1955, 1963). Pedgley (1962) referred to the trailing low pressure area behind the squall line as a wake low, a term now generally accepted for this phenomenon. However, Pedgley also could not offer an adequate explanation for the wake low. Rather, he suggested the obstacle-flow idea of Fujita (1955) as one possibility and, as another, the hypothesis put forward by Brunk (1953) that the tops of towering clouds may generate gravity waves on the tropopause, which would then produce pressure fluctuations at the ground.

sure area within which tornadoes germinate. Figure 6 contains an example of such a couplet in southeastern Colorado, but a more detailed analysis was prepared in connection with a study by Fujita (1958a) of the Illinois tornadoes of 9 April 1953 (Fig. 7). Combining time-to-space converted pressure data with 3-cm radar data, Fujita was able to demonstrate that a prominent mesolow was associated with the tornado (the hook echo in Fig. 7) and the mesohigh with the intense rainfall area to the north.

While mesoscale pressure couplets were often identified with tornadic storms, Fujita et al. (1956) observed that they could occur on a variety of scales. The small couplets were often associated with tornadoes, whereas the larger ones were found with squall mesosystems. The larger lows, first termed wake depressions by Fujita (1955) and mesolows by Fujita et al. (1956), were later called mesodepressions by Fujita (1963). As mentioned earlier, Fujita (1963) admitted that the original explanation for

An important extension of Fujita's early analyses of surface mesonetwork data was the eventual incor-

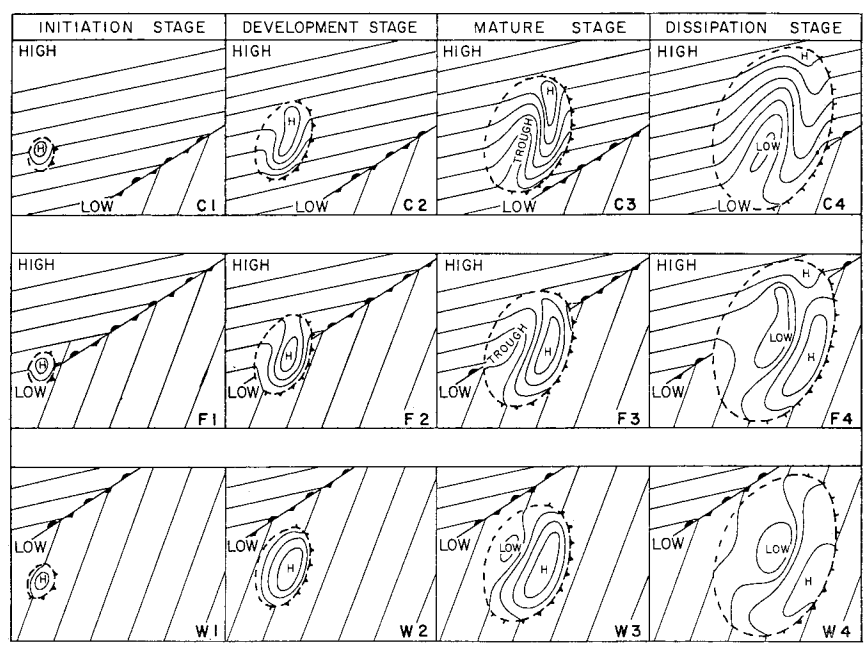

FIG. 5. Typical isobar patterns of squall mesosystems obtained by combining the basic field and excess pressure patterns. Letters C, F, and W designate the basic fields: cold sector, on the front, and warm sector, respectively. The various systems go through stages 1–4 from left to right. From Fujita (1963).

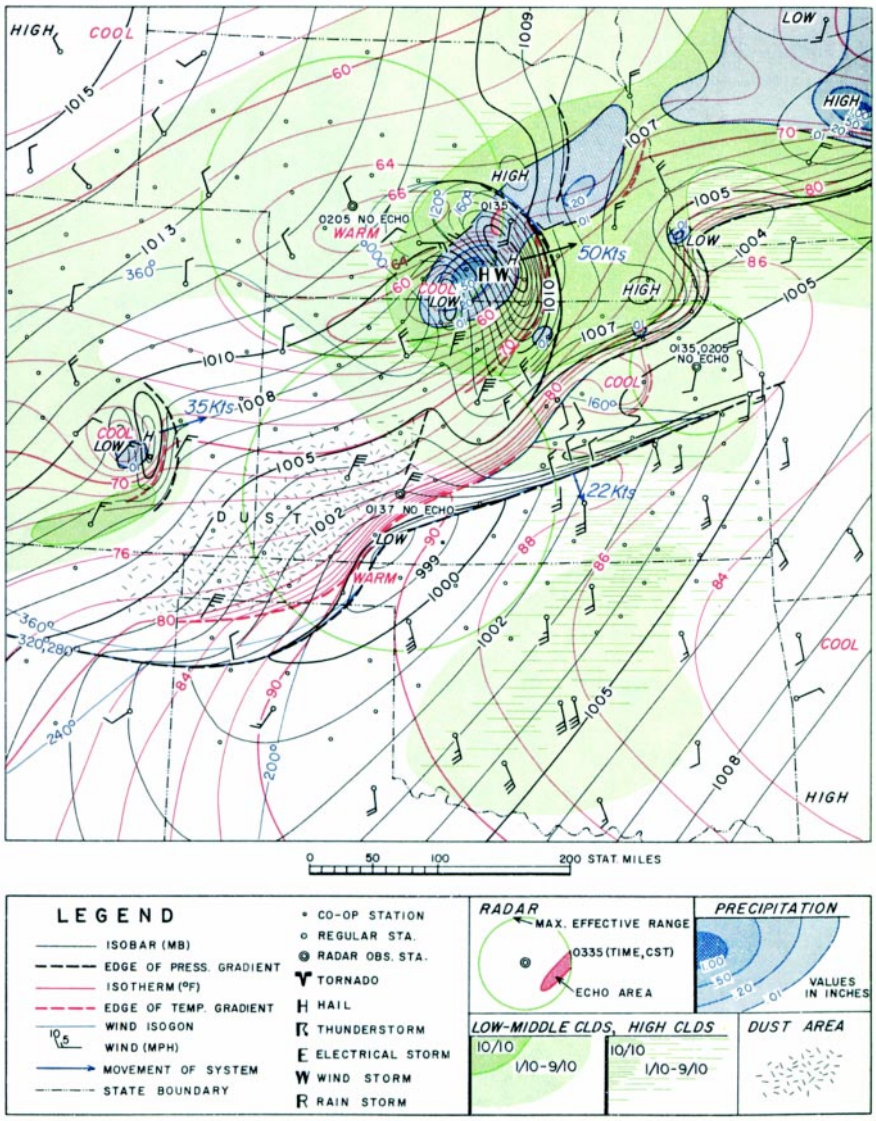

FIG. 6. Mesomap, 0200 CST 25 Jun 1953. From Fujita et al. (1956).

poration of radar data. Shown in Fig. 8 (from Fujita and Brown 1958) is a mesoanalysis in the region of the Illinois State Water Survey, Champaign, Illinois (CMI), APS-15A radar at 2200 CST on 4 June 1953. Radar echoes within the squall line approaching CMI have been added to analyses of the pressure, wind, and precipitation fields. Fujita and Brown noted that the strongest radar echoes were located in the area of the mesohigh and the lowest pressure corresponded approximately to the time of cessation of rain (isohyets are based on rain gauge data). They also found that the tracks of pressure excesses (mesohighs) and pressure deficits (wake lows) on 4–5 June deviated significantly from each other, with mesohighs generally moving toward the southeast and wake lows (which developed later) moving toward the northeast. These results are consistent with those of Pedgley (1962), who used radar and surface observations of the 1958 storm over England to document similar skew tracks of the mesohigh and wake low and similar correspondence between the precipitation and surface pressure patterns.

Fujita (1963) noted that dramatic pressure falls could occur in association with wake lows. Brunk (1949) documented a fall of 13 mb in the cold air north of a front in association with thunderstorms. The analyzed pressure pattern resembles that in Fig. 5 (upper panel). Other studies showed similar sharp pressure falls (Williams 1953, 1954; Fujita et al. 1956; Magor 1958), but the exact relationship to the precipitation structure of the convective systems was not documented. However, Williams (1963) eventually demonstrated in a quantitative way that subsidence warming can account for the observed pressure deficit in the wake low. His analysis of the thunderstorm wake of 4 May 1961 indicated a descending warm, dry current to the rear of the convective line with warm air, in this case, actually reaching the surface.[1] Williams, however, was not able to establish the cause of this circulation, nor did he investigate the relationship between the wake low and the trailing precipitation region (Fig. 4).

4. Subsequent observational studies of mesohighs and mesolows

Following a decade-long period of mesoanalytical studies that pioneered the development of mesom-

[1]Williams notes that descent of warm air all the way to the surface is not common: those areas where it does occur may experience "heat bursts" (Johnson 1983; Johnson et al. 1989).

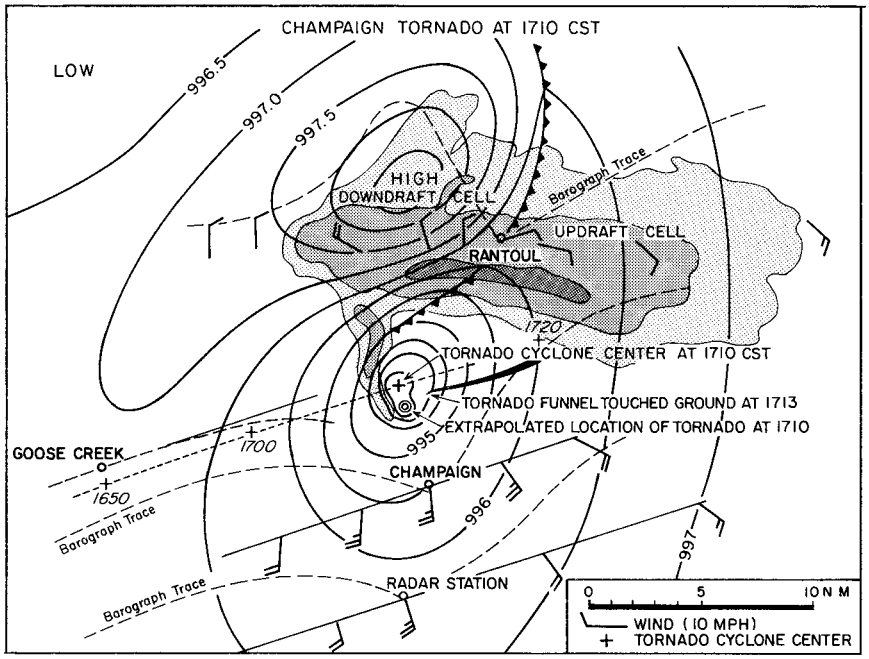

FIG. 7. Surface chart of the Champaign tornado cyclone at 1710 CST 9 Apr 1953. Redrafted from Fujita (1958).

eteorology, Fujita turned his attention in the early 1960s to several new areas of mesoscale research, notably tornadoes and satellite studies. It was left for others in following decades to further explore the ideas introduced by Fujita, and to confirm and extend many of his early findings regarding surface mesohighs and mesolows.

a. The mesohigh

Evidence from the Thunderstorm Project (Byers and Braham 1949) and the computations by Sawyer (1946) and Fujita (1959) convincingly demonstrated that the mesohigh owes its existence principally to evaporation in precipitation downdrafts. In this regard, the mesohigh can be considered primarily a hydrostatic phenomenon. However, subsequent studies have pointed out the role of specific nonhydrostatic effects. Based on instrumented tower data (Charba 1974; Goff 1976) and radar, tower, and sounding data (Wakimoto 1982; Mueller and Carbone 1987), the structures of gust fronts and mesohighs have been extensively documented. Figure 9 (from Wakimoto 1982) schematically shows the relative contributions of hydrostatic and nonhydrostatic pressure to the mesohigh for an idealized thunderstorm downdraft. At the leading edge of the outflow, the gust front, there is a buildup of nonhydrostatic pressure as a result of converging airstreams, which explains the surface pressure rises observed prior to the arrival of gust fronts. Just behind the initially elevated surge of cold air, or gust-front head, the continuing pressure rise is hydrostatic due to the dome of cold air. However, directly beneath the downdraft an additional jump in pressure occurs as a result of the nonhydrostatic effect of the downdraft impinging on the ground, leading to the pressure nose described by

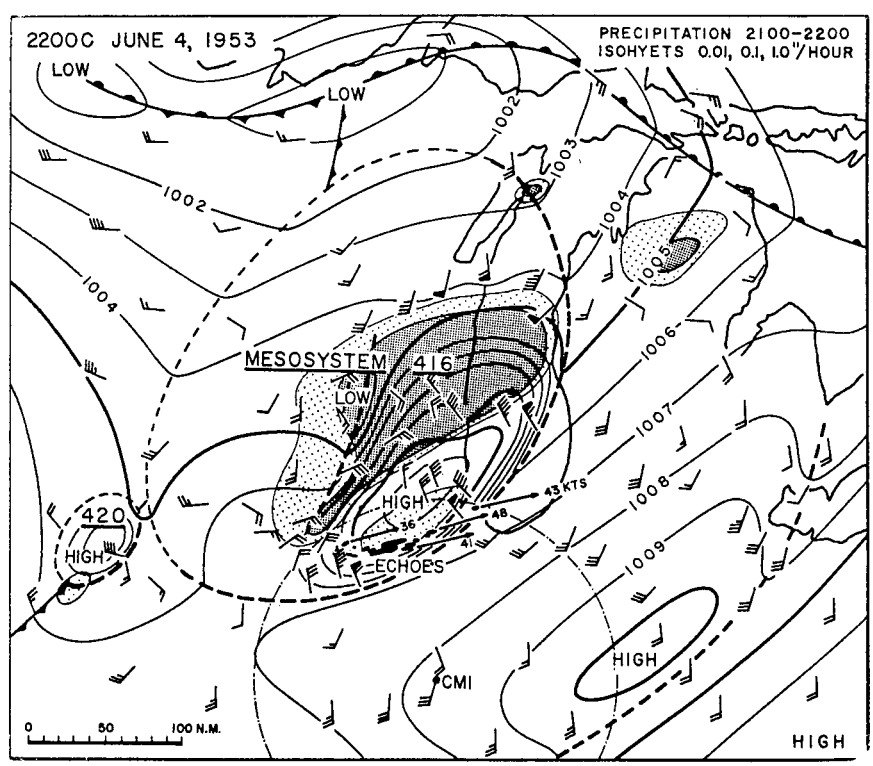

FIG. 8. Surface chart for 2200 CST 4 Jun 1953. From Fujita and Brown (1958).

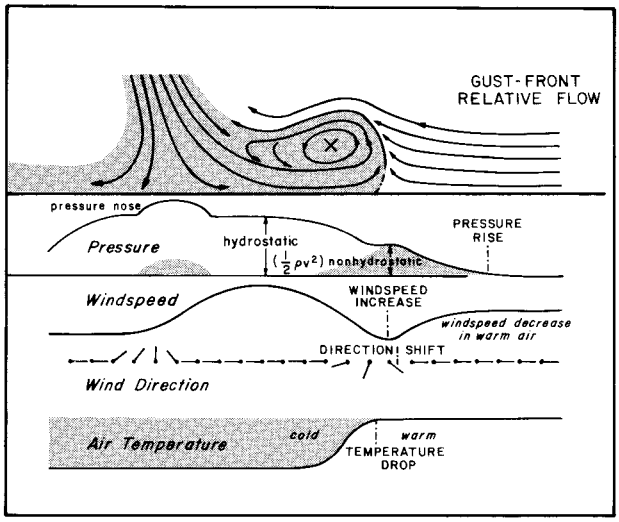

FIG. 9. Conceptual model of the surface observations during the passage of a gust front in its mature stage. From Wakimoto (1982).

Fujita (1959). An additional contribution to the mesohigh, as great as 2 mb, can arise from hydrometeor loading (Sanders and Emanuel 1977; Nicholls et al. 1988).

Since the first central and high plains surface mesonetwork of Fujita's era in the early 1950s and the National Severe Storms Project α network in the early 1960s (Fujita 1963), no network even approaching that one in areal coverage had been deployed until the 1985 Oklahoma–Kansas Preliminary Regional Experiment for STORM-Central (OK PRE-STORM). In this experiment 5-min data were collected from surface stations on a ~50 km grid over much of Kansas and Oklahoma during May and June 1985. These data elucidated the surface pressure patterns associated with mesoscale convective systems (MCSs), once again revealing the structures seen by Fujita over 30 years earlier. For example, a synthesis of analyses of these data (Fig. 10b; from Johnson and Hamilton 1988) shows the existence of a mesohigh and wake low in a squall line essentially confirming Fujita's earlier analyses.

However, improvements in radar observations, including the ability to merge data from multiple radars, have enabled placement of the surface pressure features in relation to specific components of MCSs, thereby yielding further insight into mechanisms for their development. One very common organizational mode of MCSs within which distinct surface pressure patterns are observed is the leading-line/trailing-stratiform structure (Zipser 1969, 1977; Houze 1977; Houze et al. 1989, 1990). This mode (Fig. 10b) features a leading convective line, followed by a transi-

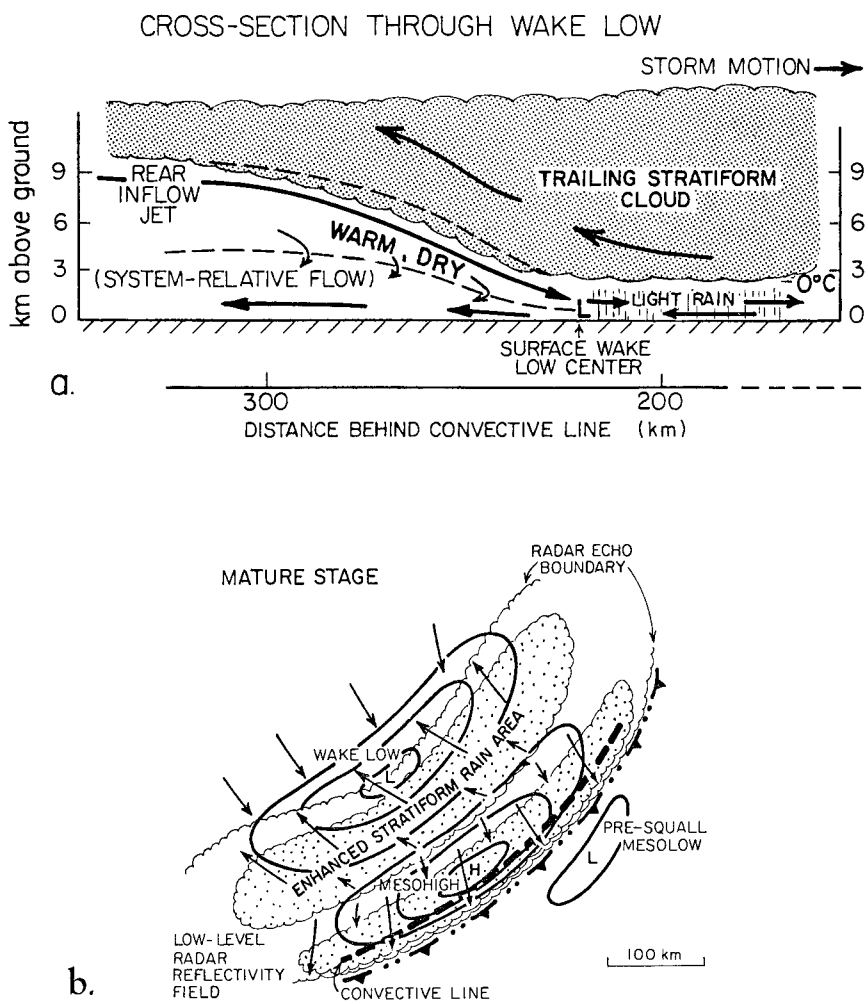

FIG. 10. Schematic cross section through the wake low at the trailing edge of (a) a squall line and (b) surface pressure and wind fields and precipitation distribution during the squall-line mature stage. Winds in (a) are system relative with the dashed line denoting zero relative wind. Arrows indicate streamlines, not trajectories, with those in (b) representing actual winds. Note that horizontal scales differ in the two schemata. From Johnson and Hamilton (1988).

tion zone (a region of minimum reflectivity), then an enhanced region of stratiform precipitation (Chong et al. 1987; Smull and Houze 1987a; Rutledge et al. 1988). The mesohigh in Fig. 10b (depicted in the mature stage of the squall line) is centered several tens of kilometers behind the leading convective line. This location suggests cumulonimbus downdrafts as a principal source for the cool mesohigh; downdrafts whose origins are hydrometeor loading and entrainment of ambient low-θ_w air from ahead of and behind the line (e.g., Newton 1950, 1966; Browning and Ludlam 1962; Zipser 1969, 1977). Later modeling studies have further emphasized the importance of the storm-relative flow from behind the system [the rear-inflow jet; Smull and Houze (1987b)] in providing a significant contribution to the mass of the surface cold pool (Fovell and Ogura 1988, 1989; Lafore and Moncrieff 1989).

Fujita (1958a) also identified smaller mesohighs associated with tornadic supercells (Fig. 7). Based on 1969–70 National Severe Storms Laboratory surface mesonetwork data having ~10 km spacing, Lemon (1976) and Barnes (1978) found the primary mesohigh to be associated with the rear-flank downdraft (RFD; Lemon and Doswell 1979), as shown schematically in Fig. 11. A weaker mesohigh was noted by Lemon (1976) near the position of the forward-flank downdraft (FFD). Both mesohighs presumably are related to evaporation of precipitation in downdrafts.

Recently, a major stride in documenting the surface pressure field in proximity to tornadoes has been achieved with an automobile-based mesonetwork (Straka et al. 1996). Figure 12 shows an example for a tornado on 2 June 1995 in Friona, Texas (P. Markowski 1999, personal communication). The pressure field based upon multiple mobile observations (each placed in correct storm-relative position using time-to-space conversion) is superposed upon the radar reflectivity field from the Doppler on Wheels (Wurman et al. 1997). This analysis, valid 5 min after tornadogenesis, is on a very fine scale in the immediate vicinity of the hook echo such that only a part of the RFD and hardly any of the FFD are sampled (cf. Figs. 7 and 11). Nevertheless, the analysis does show a strong mesolow associated with the tornado and a mesohigh associated with the RFD, consistent with Fig. 11. Although not completely sampled, there also appears on an even smaller scale (~1 km) a high pressure ring nearly enclosing the tornado, conterminous with the hook echo, as also observed by Fujita (1958b) and Rasmussen and Straka (1996).

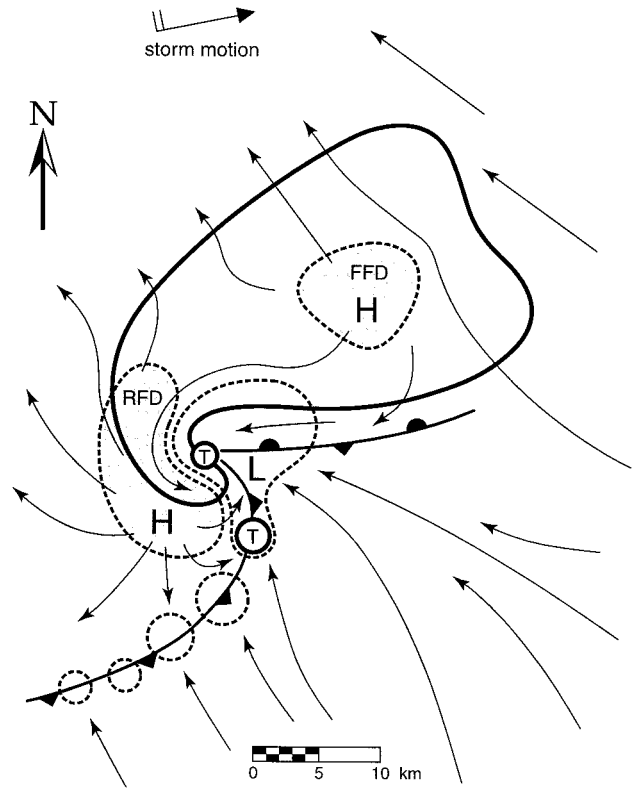

FIG. 11. Idealized surface pressure field in the region of a tornadic supercell: FFD = forward-flank downdraft, RFD = rear-flank downdraft. Echo, flow fields, and mesofronts adapted from Lemon and Doswell (1979).

b. The presquall low

Although not specifically mentioned in Fujita's papers, a presquall trough or presquall low shows up in a number of his mesoanalyses. This feature (Fig. 10b) has been attributed by Hoxit et al. (1976) to convectively induced subsidence warming in the mid- to upper troposphere ahead of squall lines. Observational studies (e.g., Fankhauser 1974; Sanders and Paine 1975; Gamache and Houze 1982; Gallus and Johnson 1991) have confirmed the existence of presquall subsidence. The modeling study of Fritsch and Chappell (1980) provided strong evidence in support of the explanation of this feature by Hoxit et al. Warm advection may also play some role in the mesolow formation (Schaefer et al. 1985), although it is likely secondary.

c. The wake low

Although the wake low for years has been clearly identified as a prominent feature of mature squall lines (Fujita 1955, 1963; Pedgley 1962), the dynamical mechanism for its formation has been elusive.

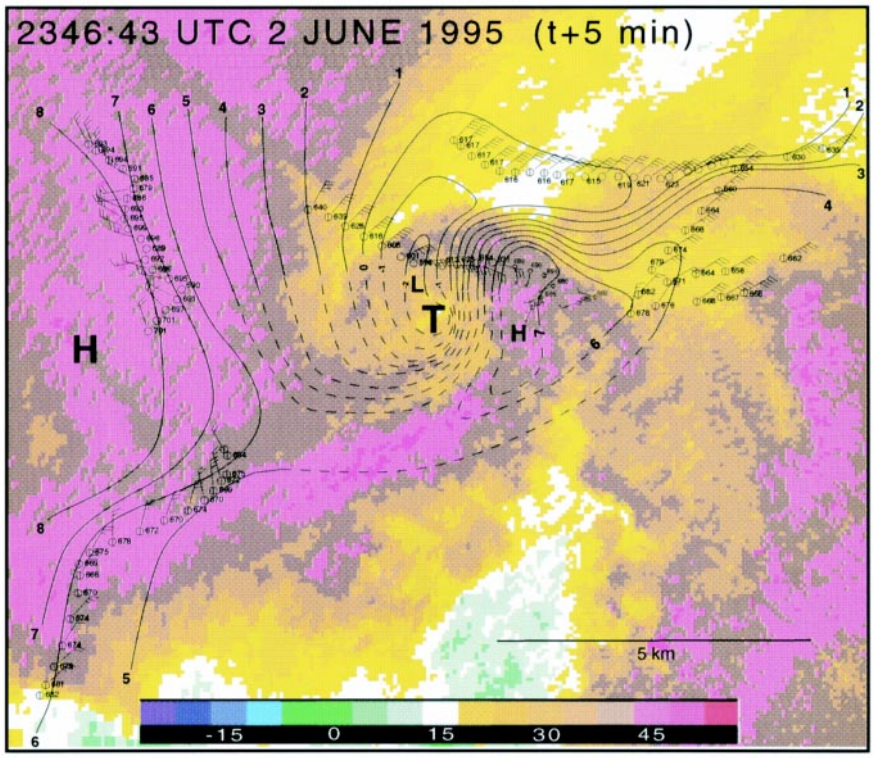

FIG. 12. Perturbation pressure field (1-mb increments, deviations from 862 mb) and radar reflectivity field (dB*Z*) at 2347 UTC 2 Jun 1995 near Friona, TX. Analysis is at 5 min after tornadogenesis (t + 5 min). Plotted pressures are in mb with hundreds digit removed: 617 = 861.7 mb. Here, *T* refers to tornado. From P. Markowski (1999, personal communication).

Williams (1963) argued that it is a consequence of subsidence to the rear of convective lines, but the processes driving the subsidence were not explained. Zipser (1969, 1977) and Brown (1979) have shown that mesoscale downdrafts driven, in part, by precipitation evaporation can lead to adiabatic warming that exceeds evaporative cooling at low levels, hence producing a pressure fall at the surface. Miller and Betts (1977) argued that the subsidence is dynamically forced by spreading cool air at the surface. The 1985 OK PRE-STORM network has allowed a more detailed evaluation of the circulations associated with wake lows. Using dual-Doppler radar data, Rutledge et al. (1988) found the rear-inflow jet to be a prominent feature of PRE-STORM squall lines. Based on a dense network of surface and sounding observations, Johnson and Hamilton (1988) hypothesized that the wake low was the surface manifestation of a descending rear-inflow jet and that the warming due to the descent was maximized at the back edge of the precipitation area where there was insufficient evaporative cooling to offset adiabatic warming (Fig. 10a). Strong warming at low levels in the descending rear-inflow jet suggests that air is overshooting its level of zero buoyancy. Dual-Doppler retrievals of the perturbation buoyancy field in the region of wake lows (Smull and Jorgensen 1990; Smull et al. 1991) have confirmed that strong overshooting at low levels (strong positive buoyancy) contributes to the intense warming there.

Fujita (1955, 1963) emphasized the life cycle characteristics of mesohighs and mesolows (Figs. 3 and 5). The depiction in Fig. 10 is for the mature stage of a squall line. In a study of 16 PRE-STORM MCSs Loehrer and Johnson (1995) found evolutions of the surface pressure fields similar to that described by Fujita. However, there tended to be an evolution of the precipitation structure of MCSs toward an *asymmetric* pattern, as defined by Houze et al. (1990): a leading convective line on the southern end and a trailing strati-

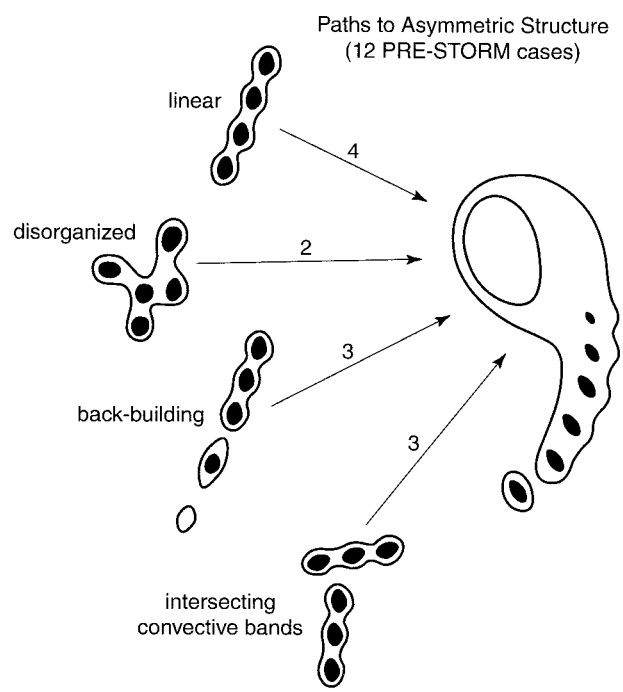

FIG. 13. Evolutionary paths to asymmetric structure for 12 MCSs during the 1985 PRE-STORM observed by Loehrer and Johnson (1995). Numbers above arrows indicate the number of systems observed to take that path. From Hilgendorf and Johnson (1998).

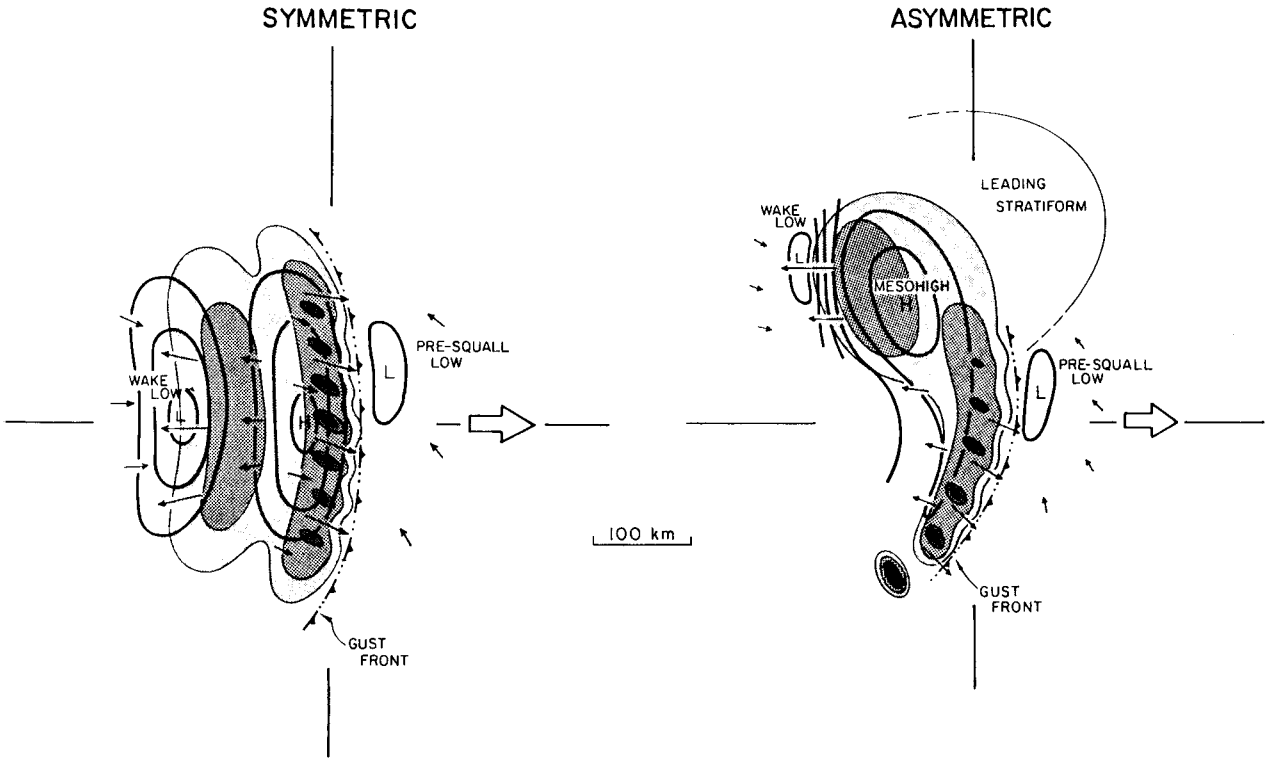

FIG. 14. Conceptual model of the surface pressure, flow, and precipitation fields associated with the (a) symmetric and (b) asymmetric stages of the MCS life cycle. Radar reflectivity field is adapted from Houze et al. (1990). Levels of shading denote increasing radar reflectivity, with darkest shading corresponding to convective cell cores. Pressure is in 1-mb increments. Small arrows represent the surface flow, lengths being proportional to the wind speed at their center. Large arrows represent the storm motion, used to define the indicated quadrants of the storm. From Loehrer and Johnson (1995).

form precipitation region to the north (Fig. 13, from Hilgendorf and Johnson 1998). Overall, four such modes were identified: broken areal, broken line and back building (after Bluestein and Jain 1985), and intersecting convective bands. During their earlier stages, some of the MCSs exhibited a *symmetric* structure, as defined by Houze et al. (1990) (left, Fig. 14). The surface pressure field during the asymmetric stage (right, Fig. 14; from Loehrer and Johnson 1995) still contains a presquall low, mesohigh, and wake low, but the wake low and, to a lesser extent, the mesohigh are shifted to the north along with the stratiform region. This shift suggests that the stratiform region plays a crucial role in forming the wake low (Stumpf et al. 1991) and plays a contributory role, along with the convective line, in forming the mesohigh. Based on a numerical modeling study, Skamarock et al. (1994) attributed MCS evolution to asymmetry to two factors: 1) the Coriolis force acting on the ascending front-to-rear flow in the convective line, turning it to the north and leading to an accumulation of hydrometeors and positively buoyant air there; and 2) the Coriolis force acting on the rear-to-front flow within the surface cold pool, driving cold air to the south and preferentially generating new cells on the southern end of the line.

Significantly, most studies of wake lows have found that they occur in association with trailing stratiform precipitation regions. When a stratiform region exists, rear-to-front flow aloft typically descends to lower levels as a result of sublimation or evaporation, or both, along the lower boundary of the stratiform cloud (Zhang and Gao 1989; Stensrud et al. 1991; Braun and Houze 1997).[2] Additionally, the mesohigh aloft that is commonly observed in MCSs (Fritsch and Maddox 1981; Maddox et al. 1981) may serve to block the upper-level flow and to channel it downward toward the leading convective line (Schmidt and Cotton 1990).

[2]Pandya and Durran (1996) showed that a realistic rear-inflow jet can occur due to thermal forcing from the leading convective line alone, although the stratiform region augments and modifies the circulation.

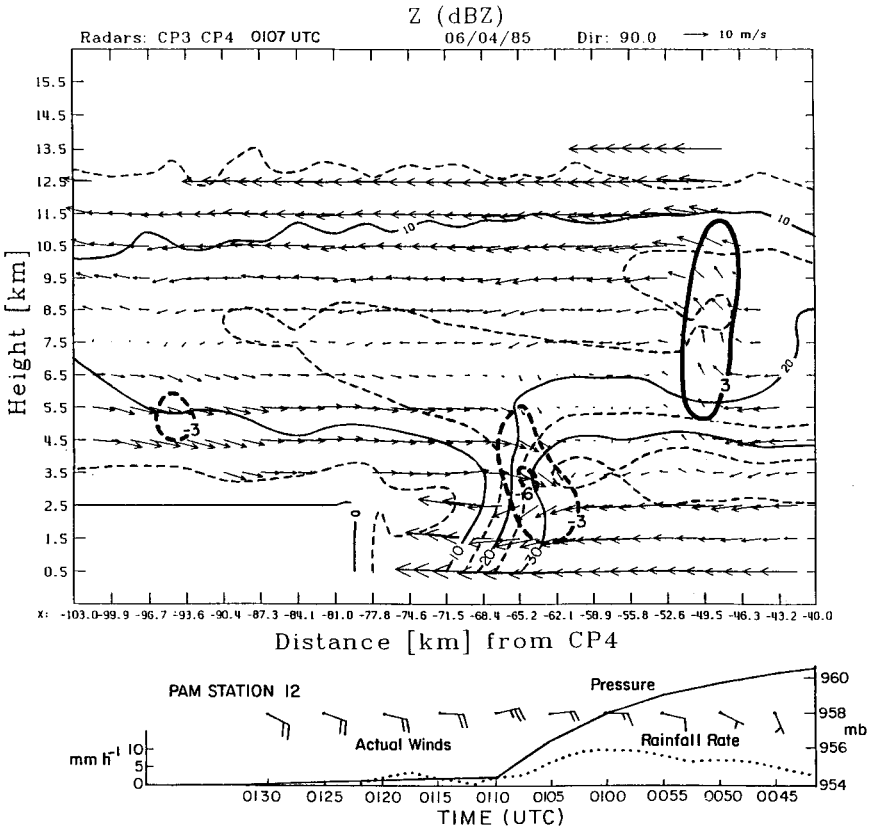

FIG. 15. Vertical cross section of radar reflectivity (dBZ) and dual-Doppler derived system-relative winds (m s^{-1}) 60 km north of National Center for Atmospheric Research CP4 radar in E–W direction across northern part of wake low domain. Vertical motion (heavy contours, 3 m s^{-1} intervals) is also indicated. In lower portion of diagram time-to-space converted observations of pressure, wind and rainfall rate at Portable Automated Mesonet Station 12 are displayed. From Stumpf et al. (1991).

A connection between descending rear-inflow jets and wake lows has been found in a number of studies. Dual-Doppler analyses for the OK PRE-STORM 3–4 and 23–24 June 1985 MCSs have revealed exceptionally rapid descent (up to 6–9 m s^{-1}) on a ~10 km scale at the rear edge of trailing stratiform regions (Stumpf et al. 1991; Johnson and Bartels 1992). An example is shown in Fig. 15 for the 3–4 June case. This section is aligned west to east (left to right) across a wake low on the left side of Fig. 15. Storm motion is toward the east and winds are system relative. Here the region of strongest descent near $x = -65$ km was coincident with the most intense gradients of surface pressure and radar reflectivity to the rear of the squall line. This downward motion, comparable to that recorded in downbursts or microbursts (Fujita and Wakimoto 1981; Fujita 1985), appears to have been a branch of the rear-inflow jet that descended rapidly as it encountered the stratiform region and experienced strong sublimation and evaporation.

Studies by Stumpf et al. (1991), Johnson and Bartels (1992), Nachamkin et al. (1994), and Loehrer and Johnson (1995) all found the most intense surface pressure gradients to be colocated with regions where the rear-inflow jet appeared to be blocked and did not continue forward through the stratiform rain area (Fig. 16, bottom; adapted from Smull et al. 1991). Stumpf et al. (1991) found that one-third of the surface pressure fall in the wake low could be attributed to a depression of the surface cold pool, as illustrated in Fig. 16 (bottom). In regions where the rear-inflow jet passes through the stratiform rain area toward the convective line, the surface pressure gradient ahead of the wake low is typically much weaker [e.g., Johnson and Hamilton (1988); Stumpf et al. (1991); see Fig. 16, top]. The causes for blocking of the rear-inflow jet in some cases and not others are not fully understood, although they may be related to stratiform precipitation intensity (Haertel and Johnson 2000) or blocking of the upper-level flow by the mesohigh aloft (Schmidt and Cotton 1990).

In some instances, the pressure gradients to the rear of the stratiform region are intense (Bosart and Seimon 1988; Loehrer and Johnson 1995; Johnson et al. 1996). One such case occurred at 0300 UTC on 6 May 1995 (Fig. 17; from Johnson et al. 1996). In this situation a mesoscale convective system was moving through east-central Oklahoma and northern Texas with a wake low at the back edge of the northern stratiform region (the southern part of the system was not captured by the Oklahoma surface mesonetwork). A mesohigh was within the region of heaviest rainfall with a deep wake low immediately to the rear of the precipitation band. The most intense pressure gradient appeared to "hug" the back edge of the stratiform rain area, consistent with the findings of Fujita and Brown (1958), Pedgley (1962), Johnson and Hamilton (1988), Stumpf et al. (1991), and Loehrer

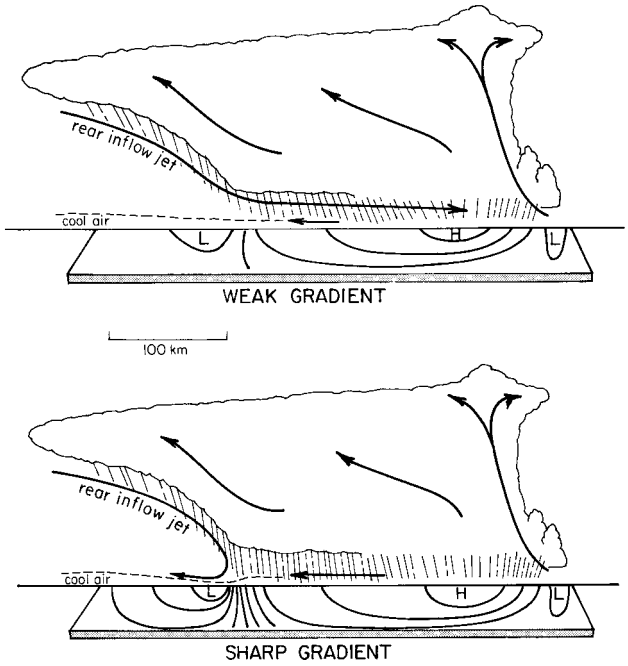

FIG. 16. Depiction of (top) weak and (bottom) sharp surface pressure gradients in association with rear-inflow jets that continue forward toward the leading convective line or are blocked, respectively.

and Johnson (1995). The most intense wake low was at the far southern boundary of the Oklahoma mesonetwork and therefore could not be fully resolved. Nevertheless, the part that was resolved revealed a pressure gradient exceeding 5 mb $(20\ km)^{-1}$: a corresponding surface pressure fall of 10 mb in 20 min! Five-minute-average surface winds within this intense gradient were 18.4 m s^{-1} from 0.92°, with a peak gust of 23.7 m s^{-1}.

The pressure gradient in Fig. 17 and those in other extreme cases that have been reported are comparable to that in the eyewall of a moderate hurricane. Although strong winds sometimes occur at the surface in these systems, they typically are not of hurricane force. The explanation is that while the surface pressure gradient may be large, its mobility and transitory behavior prevents air parcels from staying in the gradient long enough to achieve extreme velocities (Vescio and Johnson 1992). Winds are almost perpendicular to the isobars; however, the axes of divergence and convergence are displaced to the rear of the axes of the mesohigh and wake low as a result of movement of the system (Figs. 10 and 14). In some cases, as a result of reduced friction, strong and damaging winds may develop in the vicinity of wake lows that pass over open water or smooth terrain (Ely 1982). In addition, the low-level wind shear in and near the wake low poses an aviation hazard. In a survey of aircraft accidents or incidents from 1959 to 1983, Fujita and McCarthy (1990) noted that of 51 cases related to wind shear, 33 (or 65%) were associated with convective storms. Many of these were related to microbursts (Fujita and Wakimoto 1981; Fujita 1985), as discussed in a companion paper in this special issue on Fujita's work and microbursts (Wilson 2001), and some may have been connected with intense wake lows. Meuse

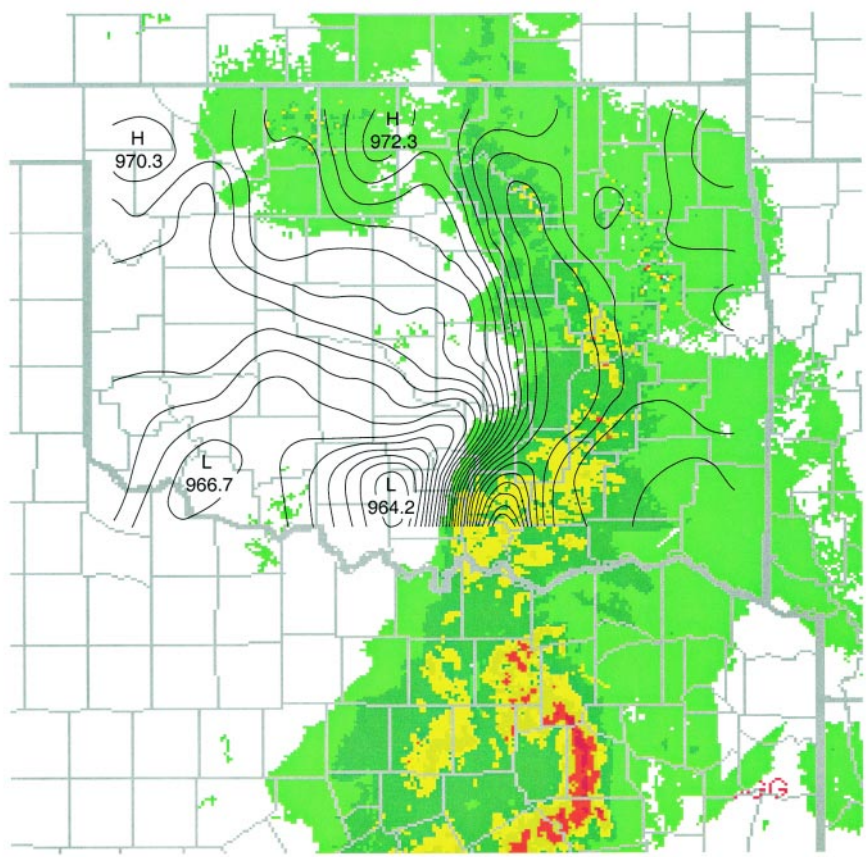

FIG. 17. Base-scan radar reflectivity at 0300 UTC 6 May 1995. Colors correspond to reflectivity thresholds of 18, 30, 41, 46, and 50 dBZ. Pressure field at 0.5-mb intervals is analyzed at 390 m (the mean station elevation). From Johnson et al. (1996).

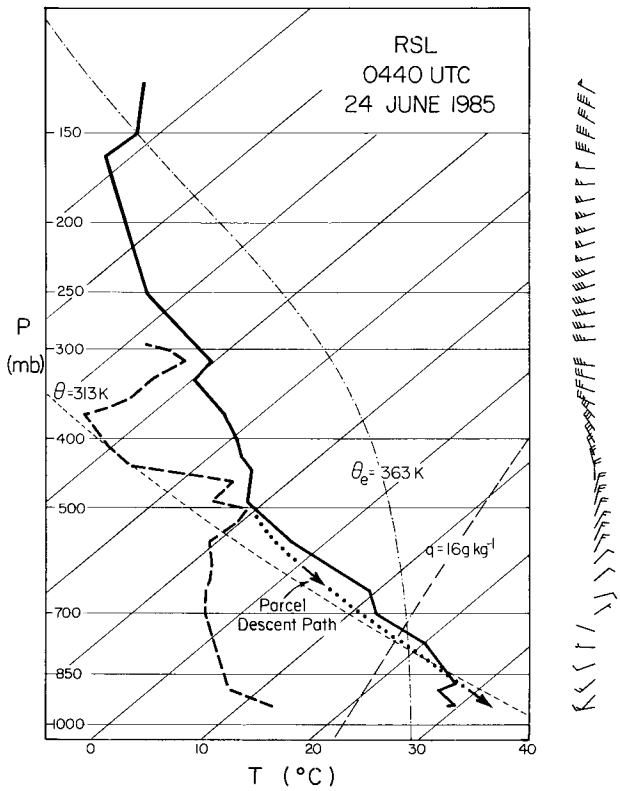

FIG. 18. Skew *T* plot for Russell, KS, at 0440 UTC 24 Jun 1985. Expected heat burst parcel trajectory is shown. Adapted from Johnson et al. (1989).

et al. (1996) reported that strong low-level wind shear near the back edge of the trailing stratiform region of a squall line nearly caused an airline crash on 12 April 1996 at the Dallas–Fort Worth International Airport.

The tendency for many MCSs to evolve from a symmetric to an asymmetric pattern with the accompanying northward shift of the stratiform region helps to explain the deviatory tracks of mesohighs and wake lows. The stratiform region appears to play a critical role in the development of a strong rear-inflow jet (Smull and Houze 1987b; Lafore and Moncrieff 1989; Weisman 1992), which in turn is linked to the formation of the wake low, as noted above. Therefore, as the stratiform region shifts northward through the life of an MCS (Hilgendorf and Johnson 1998), the wake low follows. The mesohigh, on the other hand, is coupled to both the convective line and the rear-inflow jet passing through the stratiform region. Thus, the mesohigh tracks to the right of the wake lows (Fujita and Brown 1958; Pedgley 1962; Knievel and Johnson 1998).

d. The wake low and heat bursts

In rare instances, the rapidly descending flow in an MCS reaches the surface as a hot blast of air, referred to as a heat burst. The early work by Williams (1963) actually suggested an association between rear inflow and heat bursts; however, the details of the relationship between the rear-inflow jet and cloud and precipitation structures were limited due to the sparsity of radar and sounding data. Fujita et al. (1956) noted that, in general, mesolows were associated with warm air at the surface. Observations from PRE-STORM and prior studies have provided considerably more information on the causes of heat bursts (Johnson 1983; Johnson et al. 1989; Johnson and Bartels 1992; Bernstein and Johnson 1994).

Johnson (1983) proposed that heat bursts are a consequence of strong downdrafts penetrating a shallow layer of cool air near the surface. This idea is supported by the modeling study of Proctor (1989). A sounding for the 23–24 June 1985 heat burst studied by Johnson et al. (1989) illustrates this process (Fig. 18). The lower-tropospheric structure closely resembled a dry microburst environment (Wakimoto 1985), except that a shallow, ~500 m deep stable layer existed near the surface. If an evaporating parcel were introduced from cloud base (near 500 mb), then sufficiently cooled, it could descend all the way to the surface if it had enough downward momentum to penetrate the surface stable layer. Johnson et al. (1989) found that on 23–24 June downdrafts of 6–8 m s^{-1} were sufficient to reach the surface. Later dual-Doppler analyses by Johnson and Bartels (1992) and Bernstein and Johnson (1994) confirmed that downdrafts of this magnitude existed.

There are at least two potential mechanisms for strong downdrafts and heat bursts within an MCS[3]: 1) microbursts and/or 2) rapidly descending rear- or lateral-inflow jets. Each is illustrated in Fig. 19.

First consider mechanism 1. Observations of virga or Cb mammatus led Johnson et al. (1989) to suggest that microbursts may have accounted for the intense heat bursts reported in that study. They proposed that the microbursts descending beneath virga from deep upper-level stratiform clouds (microburst type A of Fujita 1985) may have caused the heat bursts. When occurring in stratiform cloud systems to the rear of squall lines, these microbursts often descend in a nearly dry-adiabatic environment above a *deep* stable layer that has a slightly elevated moisture content near the ground. The profiles of temperature and dewpoint

[3]Of course, heat bursts can also form in association with downdrafts from isolated thunderstorms or showers penetrating a shallow surface inversion.

in these deep stable layers have been dubbed by Zipser (1977) as "onion" soundings. In most reported instances of the onion sounding, a relatively deep stable layer exists near the ground as a result of the spreading of very cool air from convective downdrafts. Microbursts impinging on such a deep stable layer typically will not have sufficient downward momentum to reach the surface (midair microbursts as defined by Fujita 1985).

In the case of a heat burst, on the other hand, this stable layer is *shallow* and the microbursts can reach the ground. Weaker microbursts may only deform the stable layer (Fig. 19, top). What makes the heat burst environment rare is not entirely clear; perhaps such a situation is favored only when mesoscale convective systems develop in relatively hot, dry conditions, as observed on this day and also reported in the heat burst study by Johnson (1983).

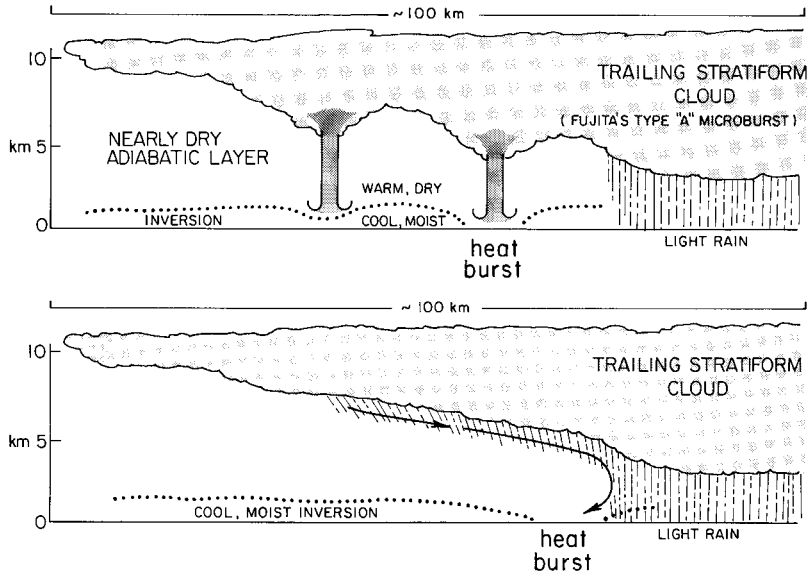

FIG. 19. Depictions of two possible heat burst mechanisms associated with the trailing stratiform regions of mesoscale convective systems: (top) microbursts penetrating shallow surface inversion and (bottom) descending rear- or lateral-inflow jet penetrating surface inversion. Heat bursts can also occur in association with downdrafts from isolated thunderstorms penetrating a surface inversion (not shown).

In mechanism 2, a rear- or lateral-inflow jet [the latter type reported in Bernstein and Johnson (1994)] descends along the edge of the stratiform precipitation region all the way to the surface (Fig. 19, bottom). This situation is similar to a microburst in the sense that sublimation and evaporation are occurring in a descending airstream (e.g., Stensrud et al. 1991), but there is a sloped trajectory toward the surface.

5. Dynamical theories for mesohighs and wake lows

Most studies have attributed squall-line mesohighs to the melting and evaporation of precipitation, which builds up a cold dome or gravity current at the surface. The propagation of the squall line is then related to gravity current dynamics where the squall-line speed is proportional to the square root of the depth of cold air times the density difference across the cold pool's leading edge. However, the gravity current concept is not completely adequate in stably stratified environments (where gravity waves should occur) nor does it explain the existence of a wake low.

While the wake low clearly is related to subsidence warming, the causes of the subsidence and overshooting are not fully understood. Zhang and Gao (1989) noted in their 2D squall-line simulation that the evaporation of precipitation in the stratiform region was necessary to develop a wake low. Gallus (1996) found in a 2D cloud model that only when the trailing stratiform precipitation region is allowed to collapse, as in the decaying phase of a squall line, does the surface pressure gradient at the back edge of the storm achieve a magnitude that approaches observations. Using a 3D, adaptive-grid cloud-resolving model, Wicker and Skamarock (1996) also found that wake lows occur at the back edge of the cold pool where the rear-inflow jet impinges upon the trailing stratiform region, but embedded within the wake low area are isolated, transitory, intense low pressure areas associated with decaying convective cells. Similar transients were documented by Knievel and Johnson (1998).

Koch et al. (1988) and Koch and Siedlarz (1999) argued that the surface pressure fields accompanying certain squall lines reflected a coupling between convection and gravity waves. They found deep convection and precipitation near the pressure maximum (mesohigh) and low pressure ahead of and behind the squall line. The coupling of convection with gravity waves was argued by Koch et al. (1988) to be in qualitative agreement with predictions from wave-CISK (conditional instability of the second kind; Lindzen 1974; Raymond 1975), wherein it is proposed that the gravity wave provides moisture convergence into the

storm and the heating/cooling distributions from the storm in turn provide the energy to drive the wave disturbance. However, it is clear from the work of Nicholls et al. (1991) and Mapes (1993) that convection excites a spectrum of gravity waves whose coupling to convection and impact on surface pressure may not have a single, simple interpretation.

An alternative theory for mesohighs and wake lows was proposed by Haertel and Johnson (2000). They simulated MCS mesohighs and wake lows using a linearized dynamical system in which the only forcing was the lower-tropospheric cooling associated with stratiform precipitation. The response consisted entirely of gravity waves, whose amplitudes were enhanced in the direction of the cool source motion. When the moving cool source (speed = 10 m s^{-1})was defined to have a three-dimensional structure, both a mesohigh and mesolow developed having characteristics and evolutions resembling squall-line mesohighs and wake lows (Fig. 20). These evolutions closely resemble those described by Fujita (1963) (cf. Fig. 5). When an upper boundary was introduced directly above the cooling, the response approached a steady state in which a mesohigh–mesolow couplet was centered on the cooling. An analytic solution showed that the large-amplitude response to *stratiform cooling* in squall lines is a unique consequence of the fact that the stratiform region's forward speed of motion typically approaches the gravity wave speed associated with the vertical wavelength of the stratiform cooling (≈13 m s^{-1} for a 4-km deep cooling). The modeled wake low intensified when the stratiform precipitation terminated (after 4 h in Fig. 20), consistent with Fujita's (1963) observations of wake low intensification during the latter stages of the life cycle of squall lines. These findings are also consistent with observations showing that wake lows tend to occur only when trailing stratiform regions exist. While the linear analysis explains the general structure of mesohigh/wake low couplets rather well, extreme pressure gradients such as those depicted in Fig. 17 are clearly influenced by nonlinear effects (e.g., rapidly descending rear-inflow jets).

6. Summary and conclusions

Much of Fujita's career was devoted to the study of surface phenomena associated with severe weather. In his early years Fujita directed most of his attention to the surface pressure, wind, and temperature patterns associated with severe storms. The analysis techniques that he developed and applied in both Japan and the United States were instrumental in the development of the field of mesometeorology.

Through time-to-space conversion of barograph data, Fujita was able to construct detailed surface maps depicting mesohighs and mesolows that accompany convective systems. On the smallest scales, he observed pressure couplets in association with tornado cyclones. On larger scales, he observed mesohighs and mesodepressions (now generally referred to as wake lows) in association with squall mesosystems several hundred kilometers in horizontal dimension. The mesohighs and wake lows exhibited a definitive life cycle: mesohighs occurred first, intensified and expanded, then wake lows developed later.

The basic surface pressure patterns accompanying severe storms defined by Fujita over 40 years ago have stood the test of time. While advances in instrumentation, notably radar, have provided greater insight into mechanisms for mesohighs and wake lows, the essential structures he proposed still remain valid. Remarkably, the physics and dynamics of these pressure features are still not completely understood. The specific roles of gravity currents and gravity waves in mesohighs and wake lows have not yet been fully resolved. Moreover, additional observational studies also are needed to better define the structure of these phenomena and, in

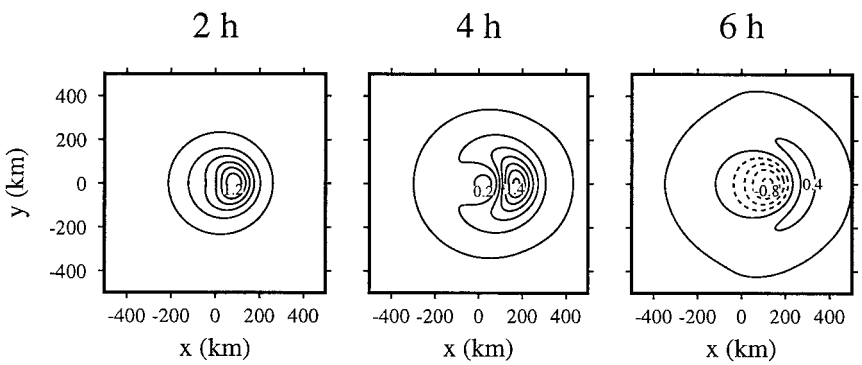

FIG. 20. The surface pressure response to a left-to-right moving, axisymmetric cooling at 2, 4, and 6 h. The forcing is chosen to represent lower-tropospheric cooling associated with the stratiform precipitation region of a squall line (width = 150 km; speed = 10 m s^{-1}; height = 4 km; lifetime = 4 h). The contour interval is 0.2 mb. From Haertel and Johnson (2000).

particular, document the meteorologically significant cases of extreme pressure gradients and high winds between mesohighs and wake lows.

Acknowledgments. This research has been supported by the National Science Foundation under Grants ATM-9313716 and ATM-9618684. I appreciate the helpful comments of Howard Bluestein, Pat Haertel and Jason Knievel; thank the latter for drafting Figs. 11, 13, and 17; and thank Paul Markowski for providing Fig. 12. Special thanks go to Kazuya Fujita for locating original versions of Figs. 1 and 2.

References

Atlas, D., R. Tatehira, R. C. Srivastava, W. Marker, and R. E. Carbone, 1969: Precipitation-induced mesoscale wind perturbations in the melting layer. *Quart. J. Roy. Meteor. Soc.*, **95,** 544–560.

Barnes, S. L., 1978: Oklahoma thunderstorms on 29–30 April 1970. Part I: Morphology of a tornadic storm. *Mon. Wea. Rev.*, **106,** 673–684.

Bernstein, B. C., and R. H. Johnson, 1994: A dual-Doppler radar study of an OK PRE-STORM heat burst event. *Mon. Wea. Rev.*, **122,** 259–273.

Bluestein, H. B., and M. H. Jain, 1985: Formation of mesoscale lines of precipitation: Severe squall lines in Oklahoma during the spring. *J. Atmos. Sci.*, **42,** 1711–1732.

Bosart, L. F., and A. Seimon, 1988: Case study of an unusually intense atmospheric gravity wave. *Mon. Wea. Rev.*, **116,** 1857–1886.

Braun, S. A., and R. A. Houze Jr., 1997: The evolution of the 10–11 June 1985 PRE-STORM squall line: Initiation, development of rear inflow, and dissipation. *Mon. Wea. Rev.*, **125,** 478–504.

Brooks, E. M., 1949: The tornado cyclone. *Weatherwise*, **2,** 32–33.

Brown, J. M., 1979: Mesoscale unsaturated downdrafts driven by rainfall evaporation: A numerical study. *J. Atmos. Sci.*, **36,** 313–338.

Browning, K. A., and F. H. Ludlam, 1962: Airflow in convective storms. *Quart. J. Roy. Meteor. Soc.*, **88,** 117–135.

Brunk, I. W., 1949: The pressure pulsation of 1 April 1944. *J. Meteor.*, **6,** 181–187.

——, 1953: Squall lines. *Bull. Amer. Meteor. Soc.*, **34,** 1–9.

Byers, H. R., 1942: Nonfrontal thunderstorms. Misc. Rep. 3, Dept. of Meteorology, University of Chicago, 26 pp. [Available from John Crerar Library, 1100 E. 57th St., University of Chicago, Chicago, IL 60637.]

——, and R. R. Braham Jr., 1949: *The Thunderstorm.* U.S. Government Printing Offices, Washington, DC, 287 pp.

Charba, J., 1974: Application of the gravity current model to analysis of squall-line gust fronts. *Mon. Wea. Rev.*, **102,** 140–156.

Chong, M., P. Amayenc, G. Scialom, and J. Testud, 1987: A tropical squall line observed during the COPT 81 experiment in west Africa. Part I: Kinematic structure inferred from dual-Doppler radar data. *Mon. Wea. Rev.*, **115,** 670–694.

Ely, G. F., 1982: Case study of a significant thunderstorm wake depression along the Texas coast: May 29–30 1981. NOAA Tech. Memo. NWS SR-105, 64 pp.

Fankhouser, J. C., 1974: The derivation of consistent fields of wind and geopotential height from mesoscale rawinsonde data. *J. Appl. Meteor.*, **13,** 637–646.

Fovell, R. G., and Y. Ogura, 1988: Numerical simulation of a midlatitude squall line in two dimensions. *J. Atmos. Sci.*, **45,** 3846–3879.

——, and ——, 1989: Effect of vertical wind shear on numerically simulated multicell storm structure. *J. Atmos. Sci.*, **46,** 3144–3176.

Fritsch, J. M., and C. F. Chappell, 1980: Numerical prediction of convectively driven mesoscale pressure systems. Part II: Mesoscale model. *J. Atmos. Sci.*, **37,** 1734–1762.

——, and R. A. Maddox, 1981: Convectively driven mesoscale pressure systems aloft. Part I: Observations. *J. Appl. Meteor.*, **20,** 9–19.

Fujita, T. T., 1951: Microanalytical study of thunder-nose. *Geophys. Mag. Tokyo*, **22,** 78–88.

——, 1955: Results of detailed synoptic studies of squall lines. *Tellus*, **7,** 405–436.

——, 1958a: Mesoanalysis of the Illinois tornadoes of April 9, 1953. *J. Meteor.*, **15,** 288–296.

——, 1958b: Tornado cyclone: The bearing system of tornadoes. *Proc. Seventh Conf. on Radar Meteorology*, Miami Beach, FL, Amer. Meteor. Soc., K31–K38.

——, 1959: Precipitation and cold air production in mesoscale thunderstorm systems. *J. Meteor.*, **16,** 454–466.

——, 1963: Analytical mesometeorology: A review. *Severe Local Storms, Meteor. Monogr.*, No. 27, Amer. Meteor. Soc., 77–125.

——, 1985: The downburst. SMRP Research Paper 210, Dept. of Geophysical Sciences, University of Chicago, 122 pp. [NTIS PB-148880.]

——, 1992: The mystery of severe storms. WRL Research Paper 239, Dept. of Geophysical Sciences, University of Chicago, 298 pp. [NTIS PB-182021.]

——, and H. A. Brown, 1958: A study of mesosystems and their radar echoes. *Bull. Amer. Meteor. Soc.*, **39,** 538–554.

——, and R. M. Wakimoto, 1981: Five scales of airflow associated with a series of downbursts on 16 July 1980. *Mon. Wea. Rev.*, **109,** 1438–1456.

——, and J. McCarthy, 1990: The application of weather radar to aviation meteorology. *Radar in Meteorology*, D. Atlas, Ed., Amer. Meteor. Soc., 657–681.

——, H. Newstein, and M. Tepper, 1956: Mesoanalysis—An important scale in the analysis of weather data. U.S. Weather Bureau Research Res. Paper 39, Washington, DC, 83 pp.

Gallus, W. A., Jr., 1996: The influence of microphysics in the formation of intense wake lows: A numerical modeling study. *Mon. Wea. Rev.*, **124,** 2267–2281.

——, and R. H. Johnson, 1991: Heat and moisture budgets of an intense midlatitude squall line. *J. Atmos. Sci.*, **48,** 122–146.

Gamache, J. F., and R. A. Houze Jr., 1982: Mesoscale air motions associated with a tropical squall line. *Mon. Wea. Rev.*, **110,** 118–135.

Goff, C. R., 1976: Vertical structure of thunderstorm outflows. *Mon. Wea. Rev.*, **104,** 1429–1440.

Haertel, P. T., and R. H. Johnson, 2000: The linear dynamics of squall-line mesohighs and wake lows. *J. Atmos. Sci.*, **57,** 93–107.

Hilgendorf, E. R., and R. H. Johnson, 1998: A study of the evolution of mesoscale convective systems using WSR-88D data. *Wea. Forecasting*, **13,** 437–452.

Houze, R. A., Jr., 1977: Structure and dynamics of a tropical squall-line system observed during GATE. *Mon. Wea. Rev.,* **105,** 1540–1567.

——, S. A. Rutledge, M. I. Biggerstaff, and B. F. Smull, 1989: Interpretation of Doppler weather radar displays of midlatitude mesoscale convective systems. *Bull. Amer. Meteor. Soc.,* **70,** 608–619.

——, B. F. Smull, and P. Dodge, 1990: Mesoscale organization of springtime rainstorms in Oklahoma. *Mon. Wea. Rev.,* **118,** 613–654.

Hoxit, L. R., C. F. Chappell, and J. M. Fritsch, 1976: formation of mesolows or pressure troughs in advance of cumulonimbus clouds. *Mon. Wea. Rev.,* **104,** 1419–1428.

Humphreys, W. J., 1929: *Physics of the Air,* McGraw-Hill, 654 pp.

Johnson, B. C., 1983: The heat burst of 29 May 1976. *Mon. Wea. Rev.,* **111,** 1776–1792.

Johnson, R. H., and P. J. Hamilton, 1988: The relationship of surface pressure features to the precipitation and air flow structure of an intense midlatitude squall line. *Mon. Wea. Rev.,* **116,** 1444–1472.

——, and D. L. Bartels, 1992: Circulations associated with a mature-to-decaying midlatitude mesoscale convective system. Part II: Upper-level features. *Mon. Wea. Rev.,* **120,** 1301–1320.

——, S. Chen, and J. J. Toth, 1989: Circulations associated with a mature-to-decaying midlatitude mesoscale convective system. Part I: Surface features—Heat bursts and mesolow development. *Mon. Wea. Rev.,* **117,** 942–959.

——, E. R. Hilgendorf, and K. C. Crawford, 1996: Study of midwestern mesoscale convective systems using new operational networks. Preprints, *18th Conf. on Severe Local Storms,* San Francisco, CA, Amer. Meteor. Soc., 308–312.

Knievel, J. C., and R. H. Johnson, 1998: Pressure transients within MCS mesohighs and wake lows. *Mon. Wea. Rev.,* **126,** 1907–1930.

Koch, S. E., and L. M. Siedlarz, 1999: Mesoscale gravity waves and their environment in the central United States during STORM-FEST. *Mon. Wea. Rev.,* **127,** 2854–2879.

——, R. E. Golus, and P. B. Dorian, 1988: A mesoscale gravity wave event observed during CCOPE. Part II: Interactions between mesoscale convective systems and antecedent waves. *Mon. Wea. Rev.,* **116,** 2545–2569.

Lafore, J.-P., and W. M. Moncrieff, 1989: A numerical investigation of the organization and interaction of the convective and stratiform regions of tropical squall lines. *J. Atmos. Sci.,* **46,** 521–544.

Lemon, L. R., 1976: The flanking line, a severe thunderstorm intensification source. *J. Atmos. Sci.,* **33,** 686–694.

——, and C. A. Doswell III, 1979: Severe thunderstorm evolution and meso-cyclone structure as related to tornadogenesis. *Mon. Wea. Rev.,* **107,** 1184–1197.

Lindzen, R. S., 1974: Wave-CISK in the tropics. *J. Atmos. Sci.,* **31,** 156–179.

Loehrer, S. M., and R. H. Johnson, 1995: Surface pressure and precipitation life cycle characteristics of PRE-STORM mesoscale convective systems. *Mon. Wea. Rev.,* **123,** 600–621.

Maddox, R. A., D. J. Perkey, and J. M. Fritsch, 1981: Evolution of upper tropospheric features during the development of a mesoscale convective complex. *J. Atmos. Sci.,* **38,** 1664–1674.

Magor, B. W., 1958: A meso-low associated with a severe storm. *Mon. Wea. Rev.,* **86,** 81–90.

Mapes, B. E., 1993: Gregarious tropical convection. *J. Atmos. Sci.,* **50,** 2026–2037.

Meuse, C., L. Galusha, M. Isaminger, M. Moore, D. Rhoda, F. Robasky, and M. Wolfson, 1996: Analysis of the 12 April 1996 wind shear incident at DFW airport. Preprints, *Workshop on Wind Shear and Wind Shear Alert Systems,* Oklahoma City, OK, Amer. Meteor. Soc., 23–33.

Miller, M. J., and A. K. Betts, 1977: Traveling convective storms over Venezuela. *Mon. Wea. Rev.,* **105,** 833–848.

Mueller, C. K., and R. E. Carbone, 1987: Dynamics of a thunderstorm outflow. *J. Atmos. Sci.,* **44,** 1879–1898.

Nachamkin, J. E., R. L. McAnelly, and W. R. Cotton, 1994: An observational analysis of a developing mesoscale convective complex. *Mon. Wea. Rev.,* **122,** 1168–1188.

Newton, C. W., 1950: Structure and mechanisms of the prefrontal squall line. *J. Meteor.,* **7,** 210–222.

——, 1966: Circulations in large sheared cumulonimbus. *Tellus,* **18,** 483–496.

Nicholls, M. E., R. H. Johnson, and W. R. Cotton, 1988: Sensitivity of two-dimensional simulations of tropical squall lines to environmental profiles. *J. Atmos. Sci.,* **45,** 3625–3649.

——, R. A. Pielke, and W. R. Cotton, 1991: Thermally forced gravity waves in an atmosphere at rest. *J. Atmos. Sci.,* **48,** 1869–1884.

Pandya, R. E., and D. R. Durran, 1996: The influence of convectively generated thermal forcing on the mesoscale circulation around squall lines. *J. Atmos. Sci.,* **53,** 2924–2951.

Pedgley, D. E., 1962: A meso-synoptic analysis of the thunderstorms on 28 August 1958. Geophysical Memo. 106, British Meteorological Office, 74 pp.

Proctor, F. H., 1989: Numerical simulation of an isolated microburst. Part II: Sensitivity experiments. *J. Atmos. Sci.,* **46,** 2143–2165.

Rasmussen, E. N., and J. M. Straka, 1996: Mobile mesonet observations of tornadoes during VORTEX-95. Preprints, *18th Conf. on Severe Local Storms,* San Francisco, CA, Amer. Meteor. Soc., 1–5.

Raymond, D. J., 1975: A model for predicting the movement of continuously propagating convective storms. *J. Atmos. Sci.,* **32,** 1308–1317.

Rutledge, S. A., R. A. Houze Jr., M. I. Biggerstaff, and T. Matejka, 1988: The Oklahoma–Kansas mesoscale convective system of 10–11 June 1985: Precipitation structure and single-Doppler radar analysis. *Mon. Wea. Rev.,* **116,** 1409–1430.

Sanders, F., and R. J. Paine, 1975: Structure and thermodynamics of an intense mesoscale convective storm in Oklahoma. *J. Atmos. Sci.,* **32,** 1563–1579.

——, and K. A. Emanuel, 1977: Momentum budget and temporal evolution of a mesoscale convective system. *J. Atmos. Sci.,* **34,** 322–330.

Sawyer, J. S., 1946: Cooling by rain as the cause of the pressure rise in convective squalls. *Quart. J. Roy. Meteor. Soc.,* **72,** 168.

Schaefer, J. T., L. R. Hoxit, and C. F. Chappell, 1985: Thunderstorms and their mesoscale environment. *Thunderstorm Morphology and Dynamics,* E. Kessler, Ed., University of Oklahoma Press, 113–130.

Schmidt, J. M., and W. R. Cotton, 1990: Interactions between upper and lower tropospheric gravity waves on squall line structure and maintenance. *J. Atmos. Sci.,* **47,** 1205–1222.

Simpson, J. E., 1987: *Gravity Currents*. Ellis Horwood Ltd., 244 pp.

Skamarock, W. C., M. L. Weisman, and J. B. Klemp, 1994: Three-dimensional evolution of simulated long-lived squall lines. *J. Atmos. Sci.,* **51,** 2563–2584.

Smull, B. F., and R. A. Houze Jr., 1987a: Dual-Doppler radar analysis of a midlatitude squall line with a trailing region of stratiform rain. *J. Atmos. Sci.,* **44,** 2128–2148.

——, and ——, 1987b: Rear inflow in squall lines with trailing stratiform precipitation. *Mon. Wea. Rev.,* **115,** 2869–2889.

—— and D. P. Jorgensen, 1990: Pressure and buoyancy perturbations near an intense wake low in a midlatitude mesoscale convective system. Preprints, *Fourth. Conf. on Mesoscale Processes,* Boulder, CO, Amer. Meteor. Soc., 214–215.

——, ——, and C. E. Hane, 1991: Comparison of retrieved pressure and buoyancy perturbations with in situ observations of an intense wake low in a midlatitude mesoscale convective system. Preprints, *25th Int. Conf. on Radar Meteorology,* Paris, France, Amer. Meteor. Soc., 135–138.

Stensrud, D. J., R. A. Maddox, and C. L. Ziegler, 1991: A sublimation-initiated mesoscale downdraft and its relation to the wind field below a precipitating anvil cloud. *Mon. Wea. Rev.,* **119,** 2124–2139.

Straka, J. M., E. N. Rasmussen, and S. E. Fredrickson, 1996: A mobile mesonet for finescale meteorological observations. *J. Atmos. Oceanic Technol.,* **13,** 921–936.

Stumpf, G. J., R. H. Johnson, and B. F. Smull, 1991: The wake low in a midlatitude mesoscale convective system having complex organization. *Mon. Wea. Rev.,* **119,** 134–158.

Suckstorff, G. A., 1935: Die strömmungsvorgänge in instabilitätschauern. *Z. Meteor.,* **25,** 449–452.

Tepper, M., 1950: A proposed mechanism of squall lines: The pressure jump line. *J. Meteor.,* **7,** 21–29.

——, 1955: On the generation of pressure-jump lines by the impulsive addition of momentum to simple current systems. *J. Meteor.,* **12,** 287–297.

Vescio, M. D., and R. H. Johnson, 1992: The surface-wind response to transient mesoscale pressure fields associated with squall lines. *Mon. Wea. Rev.,* **120,** 1837–1850.

Wakimoto, R. M., 1982: Life cycle of thunderstorm gust fronts as viewed with Doppler radar and rawinsonde data. *Mon. Wea. Rev.,* **110,** 1060–1082.

——, 1985: Forecasting dry microburst activity over the high plains. *Mon. Wea. Rev.,* **113,** 1131–1143.

Weisman, M. L., 1992: The role of convectively generated rear-inflow jets in the evolution of long-lived mesoconvective systems. *J. Atmos. Sci.,* **49,** 1826–1847.

Wicker, L. J., and W. C. Skamarock, 1996: The dynamics governing surface pressure fields in mesoscale convective systems. Preprints, *Seventh Conf. on Mesoscale Processes,* Reading, United Kingdom, Amer. Meteor. Soc., 476–478.

Williams, D. T., 1948: A surface micro-study of squall-line thunderstorms. *Mon. Wea. Rev.,* **76,** 239–246.

——, 1953: Pressure wave observations in the central Midwest, 1952. *Mon. Wea. Rev.,* **81,** 278–298.

——, 1954: A surface study of a depression-type pressure wave. *Mon. Wea. Rev.,* **82,** 289–295.

——, 1963: The thunderstorm wake of May 4, 1961. Nat. Severe Storms Project Rep. 18, U.S. Dept. of Commerce, Washington, DC, 23 pp. [NTIS PB-168223.]

Wilson, J. W., 2001: The discovery of the downburst: T. T. Fujita's contribution. *Bull. Amer. Meteor. Soc.,* **82,** 49–62.

Wurman, J., J. M. Straka, E. N. Rasmussen, M. Randall, and A. Zahrai, 1997: Design and deployment of a portable, pencil-beam, pulsed, 3-cm Doppler radar. *J. Atmos. Oceanic Technol.,* **14,** 1502–1512.

Zhang, D.-L., and K. Gao, 1989: Numerical simulation of an intense squall line during 10–11 June 1985 PRE-STORM. Part II: Rear inflow, surface pressure perturbations and stratiform precipitation. *Mon. Wea. Rev.,* **117,** 2067–2094.

Zipser, E. J., 1969: The role of organized unsaturated downdrafts in the structure and rapid decay of an equatorial disturbance. *J. Appl. Meteor.,* **8,** 799–814.

——, 1977: Mesoscale and convective-scale downdrafts as distinct components of squall-line circulation. *Mon. Wea. Rev.,* **105,** 1568–1589.